Water and Proton Transport

Deutsche Ausgabe: DOI: 10.1002/ange.201600219
Internationale Ausgabe: DOI: 10.1002/anie.201600219

Nanoscale Distribution of Sulfonic Acid Groups Determines Structure and Binding of Water in Nafion Membranes

Xiao Ling, Mischa Bonn, Sapun H. Parekh, and Katrin F. Domke**

Abstract: *The connection between the nanoscale structure of two chemically equivalent, yet morphologically distinct Nafion fuel-cell membranes and their macroscopic chemical properties is demonstrated. Quantification of the chemical interactions between water and Nafion reveals that extruded membranes have smaller water channels with a reduced sulfonic acid head group density compared to dispersion-cast membranes. As a result, a disproportionally large amount of non-bulk water molecules exists in extruded membranes, which also exhibit larger proton conductivity and larger water mobility compared to cast membranes. The differences in the physicochemical properties of the membranes, that is, the chemical constitution of the water channels and the local water structure, and the accompanying differences in macroscopic water and proton transport suggest that the chemistry of nanoscale channels is an important, yet largely overlooked parameter that influences the functionality of fuel-cell membranes.*

Proton-exchange-membrane (PEM) fuel cells are attractive candidates for alternative energy conversion schemes because they provide high energy densities at practically zero greenhouse gas emissions. Tremendous efforts are aimed at developing improved PEMs with increased proton transport efficiencies. Such efforts require fundamental knowledge of the physical chemistry that governs transport in these materials.[1] One established route towards PEMs with high proton diffusivity is modification of the chemical composition of the PEM polymer matrix, for instance by incorporation of hydrophilic or hygroscopic additives into the PEM.[1a,2] The interactions between functional groups in the membrane matrix and water molecules are known to directly affect proton conductivity and thus are intimately linked with PEM-fuel-cell performance.[1b,3] Similarly, membrane topology, particularly the pore tortuosity, plays an important role for achieving efficient transport of water and protons across the PEM and is also a strategic target for PEM engineering.[4] In addition to chemical composition and membrane topology, the nanoscale chemical constitution of water channels, that is, how functional head groups are distributed across them, should also directly affect membrane–water chemistry, and therefore transport properties, in PEMs;[5] however, experimental proof of this effect is scarce.[5,6]

In this work, we quantify chemical interactions between water and Nafion in two membranes with the same chemical composition (and equivalent weight, EW) that have been cast in different ways by using nonlinear Raman spectroscopy. Our results show that the molecular environment in the nanochannels of these two compositionally identical, but differently processed Nafion membranes is distinct under fully hydrated conditions, where proton conductivity is maximized. Water channels in the two membranes exhibit distinct chemical constitutions that modulate the water–membrane chemistry beyond what is expected based purely on geometrical changes in channel morphology. Interestingly, a disproportional increase in undercoordinated water molecules in membranes with smaller channel diameters correlates with improved macroscopic water and proton transport properties under the same conditions.

In this study, we used two chemically identical (N117 and N212; EW = 1100 g), but differently processed (N117: extruded, N212: solution-cast) commercial Nafion membranes.[7] Nafion membranes are the most widely used and studied PEMs because of their superior chemical and thermal stability and transport properties.[8] Nafion consists of hydrophobic Teflon backbones and ether-linked side chains terminated with hydrophilic sulfonic acid head groups. It is commonly accepted that hydrophilic–hydrophobic phase separation results in the formation of ionic water channels[8] of a few nanometers in diameter or thickness that are distributed in the hydrophobic Teflon network.

Using broadband coherent anti-Stokes Raman scattering (CARS) spectroscopy (a nonlinear analogue of Raman spectroscopy),[9] we measured vibrational spectra of fully hydrated Nafion membranes. Figure 1 shows the processed CARS spectra obtained from an about 1 μm^3 voxel within fully hydrated N117 (green) and N212 (black) normalized to the CF_2 stretching band intensity of the Teflon backbone (Figure 1, right). The intensities in processed CARS spectra are directly proportional to the concentration of vibrational moieties in the focal volume, and thus allow for quantitative band analysis. A detailed description of the experimental and data-processing procedures can be found in the Supporting Information (SI). The membranes are mounted in a homebuilt microfluidic sample holder that ensures complete hydration of the membrane during acquisition (Figure 1, left). To demonstrate the applicability of our in situ spectroscopic

[*] X. Ling, Prof. Dr. M. Bonn, Dr. S. H. Parekh, Dr. K. F. Domke
Department of Molecular Spectroscopy
Max-Planck-Institut für Polymerforschung
Ackermannweg 10, 55128 Mainz (Germany)
E-mail: parekh@mpip-mainz.mpg.de
domke@mpip-mainz.mpg.de

Supporting information for this article (details about experiments and data analysis) can be found under http://dx.doi.org/10.1002/anie.201600219.

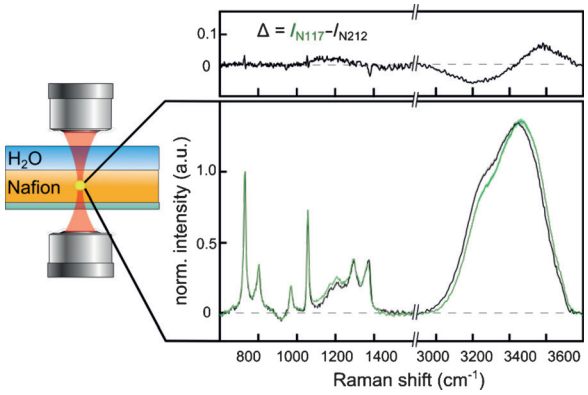

Figure 1. Left: Sketch of a forward-scattering CARS experiment. Right bottom: Processed CARS spectra from fully hydrated N212 (black) and N117 (green) Nafion membranes. Variability from three different membrane slices of the same batch is shown as shadows to the solid-line spectra. Right top: Difference spectrum $I_{N212}-I_{N117}$.

technique for Nafion systems, we extracted an apparent diffusion coefficient (ADC) for water permeating through fully hydrated membranes from time-lapsed CARS spectra (Figure S1). The observed water diffusivities for N117 ($ADC_{117} = 5.3\times10^{-10}$ m^2s^{-1}) and N212 ($ADC_{212} = 3.6\times10^{-10}$ m^2s^{-1}) are quantitatively consistent with those previously measured with NMR spectroscopy by other groups for extruded and solution-cast membranes of similar properties, and are statistically significant ($p < 0.05$, Table S1).[4b]

The spectra of N117 and N212 are nearly identical in the fingerprint region (700 to 1600 cm^{-1}), which contains prominent Nafion stretching vibrations arising from CF_2, CS, COC, and SO_3^- at 731, 803, 970, and 1057 cm^{-1}, respectively.[10] The difference spectrum ($I_{N117}-I_{N212}$; Figure 1, top) shows that all Nafion band positions and relative intensities are virtually indistinguishable for N117 and N212, as one might expect for identical EW polymers of the same chemical composition. The slight deviation between 1100 and 1250 cm^{-1} arises from imperfect error-phase correction in our data-processing routine and is not considered further in this work.[11]

At higher wavenumbers, the spectra show a broad response from the OH stretching of water that extends from ca. 3000 to 3700 cm^{-1}. The broad OH peak from N117 appears blue-shifted with respect to that from N212 as seen from the dispersive lineshape in the difference spectrum. Integration of the CF_2-normalized OH band over the entire range in N117 and N212 yields the same total band intensity to within 2.5%. The variation of the Raman scattering cross section with frequency is relatively weak and the spectral shift is only 50 cm^{-1}, so direct integration is reasonable (SI).[12] Therefore, the total number of OH groups (typically extrapolated to the number of water molecules) per CF_2 group is essentially identical for both samples. However, the peak shift and different spectral shape clearly indicate two different chemical environments of the water molecules in N117 and N212.

To gain insight into the differences in the chemical interactions between water and Nafion and to identify the contributions of different water species, that is, water molecules in different chemical environments, to the total OH stretching signal, we decomposed the OH region using a constrained classical least-squares (CCLS) fitting routine.[13] As a starting point, we assumed that water molecules inside fully hydrated Nafion either 1) are completely surrounded by—and hydrogen-bonded to—other water molecules ("bulk-like water", bulkW), or 2) interact (at least partially) with the Nafion membrane and therefore less with other water molecules, which we term undercoordinated non-bulk water (nonbulkW).[3] Other water species may exist, but starting with a minimum number of two components was reasonable to determine the appropriate number of subspecies that make up the total signal, in line with other work on Nafion–water interaction.[4b]

The CCLS fitting routine employed a global fit to both N117 and N212 spectra with two component spectra: 1) a common reference spectrum from a water reservoir for bulkW and 2) a common nonbulkW spectrum that was deduced in the fitting process itself (Figure S2). This CCLS fitting approach constrained both N212 and N117 to contain the same two subspecies of water and produced a unique nonbulkW spectrum, as well as the fractional contributions of the bulkW and nonbulkW components to the total OH spectral intensity in each membrane.

The results of the CCLS fitting are shown in Figure 2. The deduced nonbulkW component has its peak maximum at

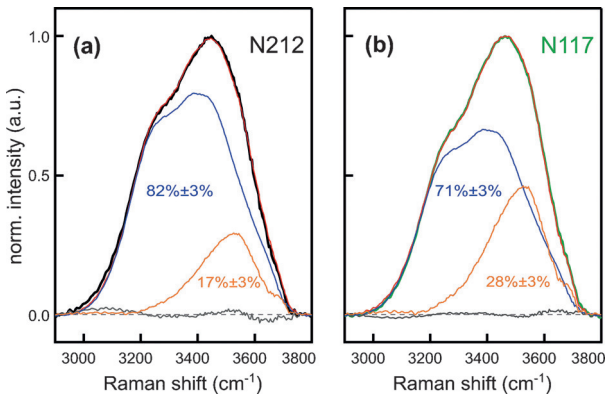

Figure 2. Relative contributions of bulk (blue) and non-bulk (orange) OH intensities to the overall OH stretching signal of N212 (a, black) and N117 (b, green) as obtained from CCLS fitting. Red: CCLS fit to the overall OH signal. Gray: fitting residual. The uncertainty in the percentages comes from three independent measurements on three different samples.

3530 cm^{-1} with a shoulder at 3678 cm^{-1}. Such high-wavenumber OH stretching bands are typically assigned to water molecules that are not tetrahedrally coordinated to four other water molecules (as is the case for bulkW molecules).[14] Prominent examples for such undercoordinated OH groups are those of water in vapor, or in contact with hydrophobic interfaces, where one of the two OH bonds of water molecules experiences less hydrogen-bonding to other water molecules.[14a,15] The shape of the nonbulkW spectrum obtained from CCLS fitting resembles reference spectra recorded from an aqueous solution of perfluorobutanesulfonic acid and from air-dried Nafion (Figure S3). Moreover, the shoulder at

3678 cm^{-1} is reminiscent of non-hydrogen-bound OH species.[12] Taken together, these observations strongly suggest that the nonbulkW is undercoordinated water located in proximity to the SO_3^- and CF_2 moieties of the membrane.

The overall water response from both N212 (Figure 2a, black) and N117 (Figure 2b, green) are fit excellently using the input spectrum from bulkW and the nonbulkW spectrum obtained from the CCLS fit as shown by the residual (gray) in Figure 2 with a root-mean-squared error of less than 1% over the fitting range for both membranes. Figure 2 shows that the fractional contribution of bulkW to the total amount of water is significantly smaller in N117 (71%) than in N212 (82%) while that of the nonbulkW species is correspondingly higher in N117 than in N212. The ± values in Figure 2 are the standard deviations of the contribution of the bulkW and nonbulkW from three different measurements based on doing the fit for each spectrum. The higher contribution of nonbulkW in N117 indicates a larger amount of undercoordinated water molecules that are presumably in contact with the sulfonic acid head groups and/or the hydrophobic Teflon backbone of the membrane.

The fitting results raised an interesting question: how can two Nafion membranes with identical chemical composition, that is, chemically identical in EW and spectroscopically, have different relative contributions of bulk and non-bulk water? Molecular dynamics (MD) simulations have suggested that nanoscale physicochemical properties, for example, the size[4a,8] and chemical constitution[5] of water channels and hydrophobic domains, play a crucial role for the overall physicochemical properties of PEMs, in addition to the macroscale membrane chemistry and pore connectivity of water channels. However, direct experimental proof relating nanoscale chemical constitution with membrane physical chemistry for Nafion is scarce.[5,6]

Small-angle scattering experiments (SAXS/SANS) have shown the radius of cylindrical water channels to be 5–20% smaller in extruded than in solution-cast hydrated Nafion of 1100 g EW.[7c,16] It follows that the circumference of an idealized, cylindrical channel (as well as the channel surface area) is accordingly 5–20% larger for N212 compared to N117. Thus, the area-to-volume (A/V) ratio of the channel surface is 5–20% larger for N117, assuming the total length of the channels is the same and much larger than the channel radius in both membranes. Recall that the spectra from the two fully hydrated membranes (Figure 1) show the same concentrations of Nafion (SO_3^- and COC moieties) and water (integrated OH) per CF_2 group within the focal volume. Combining our spectroscopy data with the SAXS/SANS results, we can deduce relative differences in the nanoscale physicochemical architecture of the two Nafion membranes. Since the water channels in N117 are smaller than those in N212, but both membranes show the same concentration of Nafion and water, N212 must contain fewer water channels of larger diameter and have a larger surface density of sulfonic acid head groups (SO_3^- surface density). Conversely, N117 contains more, but smaller water channels with a lower SO_3^- surface density across the water-channel surface compared to N212. These nano-architectural differences in the chemical constitution of N117 and N212 are schematically depicted in Figure 3.

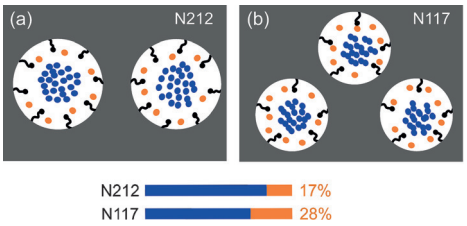

Figure 3. Schematic cross sections of the different nanoscale chemical constitutions of N212 (a) and N117 (b) water channels. The total amount of water and the relative water-to-Nafion concentrations are the same for both membranes within the slab, that is, the focal volume. Blue: bulk water; orange: non-bulk water; black: SO_3^-/COC groups; gray: Teflon backbone.

Let us now return to the different water spectra from the fully hydrated N117 and N212 membranes. The relative amounts of bulkW and nonbulkW as extracted by CCLS fitting (Figure 2) for each membrane are qualitatively consistent with the architectural differences proposed above for the two membranes. The smaller water-channel diameter (and thus larger A/V ratio) in N117 accommodates less bulkW species, favoring nonbulkW, that is, water molecules that are in contact with the channel surface (with hydrophilic SO_3^- head group and/or hydrophobic polymer backbone) rather than with each other.

By assuming a core–shell model for the water in the channel where bulkW is core water and nonbulkW is shell water, our spectroscopic data allowed us to quantitatively assess the thickness of the nonbulkW shell in N117 and N212 under fully hydrated conditions. Such a core–shell model was successfully employed to describe the chemistry and vibrational population dynamics of water in nano-emulsions of 1.7 to 28 nm in diameter, which is similar to the size of the Nafion channels.[17]

In our analysis, I_{nbw} (contribution of nonbulkW component) and I_{bw} (contribution of bulkW component) are fractional quantities of the total OH spectral intensity ($I_{nbw} + I_{bw} = 1$). Each quantity is proportional to the percentages of nonbulkW and bulkW molecules, respectively, which themselves are further proportional to the fractional volume of shell (nonbulkW) and core (bulkW) water in the channels, respectively (assuming a constant water density). This allowed writing the nonbulkW contribution as $I_{nbw}/(I_{nbw} + I_{bw}) = (V_t - V_{core})/V_t$, where V_t and V_{core} are the total channel volume and the core water volume in the channels, respectively. Plugging in formulas for core–shell cylindrical channels, we arrive at $I_{nbw} = (2r_c\, t - t^2)/r_c^2$, where r_c and t are the channel radius and shell thickness, respectively. Since we know I_{nbw} from our measurements, we can estimate the thickness of shell water in the two Nafion membranes. Starting with N212 where $I_{nbw} = 0.17$ and assuming $r_c^{212} \approx 2.3$ nm (the average of SAXS measurements),[7c,16] we calculated $t_{N212} = 0.2$ nm, corresponding to roughly 0.5 water molecules (with a molecular radius of water of 0.19 nm, calculated from a density of 1 g mL^{-1}).

SAXS/SANS studies report an average water channel size for N117, r_c^{117}, of about 2 nm.[7c,16] The same calculation for N117 ($I_{nbw} = 0.28$) revealed a shell thickness of 0.3 nm, or 50% larger than that of N212. An analogous calculation for a flat channel structure, as suggested by Kreuer and Portale,[8b] yielded a similar result: the thickness of nonbulkW in N117 is about 1.5 water molecules vs about 1 water molecule for N212 (Figure S4). This increase in shell thickness for N117 can be explained by a change in the chemistry of the water channel surface. Recalling that the concentration of SO_3^- groups is the same in N117 and N212, and that channels in N117 are smaller than in N212, the SO_3^- surface density in N117 must be lower than in N212 (Figure 3). Apparently, the decrease in SO_3^- surface density accompanying the reduction in water channel size in N117 causes an increase in the thickness of shell water. This change in the water arrangement likely contributes to differences in water and proton transport between the two materials (Table S1).

There have been few attempts to understand how membrane nanoscale architecture affects the (macroscopic) water and proton transport properties of PEMs.[4a,6b,18] In a full atomistic MD simulation, Jang et al. showed that different chemical constitutions, that is, different spatial distributions of the same number of SO_3^- groups along polymer backbones, in N117 membranes of the same EW had a strong influence on the proton and water transport properties. They found enhanced water transport in nanostructures with segregated (nonuniformly distributed) hydrophilic domains, compared with hydrophilic domains that are equally spaced along the polymer.[5a] Our results reveal a lower SO_3^- surface density—larger distance between hydrophilic groups—and a faster macroscopic water transport in N117 compared to N212. From our measured macroscopic ADCs and volume fractions of bulkW and nonbulkW in both membranes, we can estimate an ADC for each water component. Assuming that the macroscopic ADC is a linear combination of diffusion from each water component, with $ADC_w = ADC_{bw} \times I_{bw} + ADC_{nbw} \times I_{nbw}$,[19] we obtain $ADC_{bw} \approx 1 \times 10^{-10}\ m^2 s^{-1}$ and $ADC_{nbw} \approx 16 \times 10^{-10}\ m^2 s^{-1}$, for both N117 and N212. These numbers are consistent with the general trend that undercoordinated water is less hindered.[6b] Thus, changing the SO_3^- surface density leads to a disproportional change of the amount rather than of the mobility of nonbulkW. However, we note that this estimation is oversimplified by assuming a single type of nonbulkW (as represented by the *same* spectral response), which does not allow for different nonbulkW subspecies to exist and diffuse at different rates, which would be necessary to directly test Jang's theory. Further experiments to investigate the dynamics of nonbulkW subspecies are currently underway in our laboratory.

To summarize, nanoscale chemical constitution and corresponding molecular-scale water–membrane interaction, in addition to morphology, are significantly different for extruded (N117) and solution-cast (N212) membranes with the same EW polymer. An increase in the amount of non-bulk water beyond that expected from geometry (channel size reduction) alone necessitates, in the context of a core–shell model, a thicker shell of undercoordinated water in N117. Interestingly, N117 also exhibits faster water and proton transport compared to N212. The extent to which the observed transport properties result from nanoscale architectural changes and subsequent differences in water–membrane interactions, or from channel tortuosity and alignment is an unresolved question that certainly requires further investigation. Nevertheless, our results highlight that future theoretical and experimental studies comparing different PEMs should include parameters that capture the impact of nanoscale channel architecture on physical chemistry to accurately interpret the underlying physics of water and proton transport in PEMs.

Acknowledgements

We gratefully acknowledge M. J. Van Zadel, F. Fleissner, and J. Hunger for general technical and scientific support and Anke Kaltbeitzel for proton-conductivity measurements. K.F.D. acknowledges generous support through the Emmy Noether program of the German Research Foundation (DFG) #DO 1691/1-1. X.L. and K.F.D. acknowledge funding through EU FP7 (ITN-FINON #607842). S.H.P. acknowledges funding from the DFG #PA 252611-1 and the Marie Curie Foundation #CIG322284.

Keywords: chemical constitution · CARS · membrane nanostructures · Nafion · proton exchange membranes

How to cite: *Angew. Chem. Int. Ed.* **2016**, *55*, 4011–4015
Angew. Chem. **2016**, *128*, 4079–4083

[1] a) S. J. Peighambardoust, S. Rowshanzamir, M. Amjadi, *Int. J. Hydrogen Energy* **2010**, *35*, 9349–9384; b) M. A. Hickner, B. S. Pivovar, *Fuel Cells* **2005**, *5*, 213–229.
[2] Y. Zhang, J. Li, L. Ma, W. Cai, H. Cheng, *Energy Technol.* **2015**, *3*, 675–691.
[3] M. Falk, *Can. J. Chem.* **1980**, *58*, 1495–1501.
[4] a) K. D. Kreuer, *J. Membr. Sci.* **2001**, *185*, 29–39; b) Q. Zhao, P. Majsztrik, J. Benziger, *J. Phys. Chem. B* **2011**, *115*, 2717–2727.
[5] a) S. S. Jang, V. Molinero, C. Tahir, W. A. Goddard, *J. Phys. Chem. B* **2004**, *108*, 3149–3157; b) M. T. McDonnell, D. J. Keffer, *Microporous Mesoporous Mater.* **2013**, *177*, 17–24.
[6] a) R. Devanathan, *Energy Environ. Sci.* **2008**, *1*, 101–109; b) J. Song, O. H. Han, S. Han, *Angew. Chem. Int. Ed.* **2015**, *54*, 3615–3620; *Angew. Chem.* **2015**, *127*, 3686–3691.
[7] a) DuPont, Nafion® PFSA Membranes N117 Datasheet; b) DuPont, Nafion® PFSA Membranes NR211 and NR212 Datasheet; c) M. Kim, C. J. Glinka, S. A. Grot, W. G. Grot, *Macromolecules* **2006**, *39*, 4775–4787.
[8] a) K. Schmidt-Rohr, Q. Chen, *Nat. Mater.* **2008**, *7*, 75–83; b) K.-D. Kreuer, G. Portale, *Adv. Funct. Mater.* **2013**, *23*, 5390–5397.
[9] Y. Liu, Y. J. Lee, M. T. Cicerone, *Opt. Lett.* **2009**, *34*, 1363–1365.
[10] A. Gruger, A. Régis, T. Schmatko, P. Colomban, *Vib. Spectrosc.* **2001**, *26*, 215–225.
[11] C. H. Camp, Y. J. Lee, M. T. Cicerone, *J. Raman Spectrosc.* **2015**, DOI 10.1002/jrs.4824.
[12] S. A. Corcelli, J. L. Skinner, *J. Phys. Chem. A* **2005**, *109*, 6154–6165.
[13] K. F. Domke, T. A. Riemer, G. Rago, A. N. Parvulescu, P. C. A. Bruijnincx, A. Enejder, B. M. Weckhuysen, M. Bonn, *J. Am. Chem. Soc.* **2012**, *134*, 1124–1129.

[14] a) Q. Du, E. Freysz, Y. R. Shent, *Science* **1994**, *264*, 826 – 828; b) Q. Du, R. Superfine, E. Freysz, Y. Shen, *Phys. Rev. Lett.* **1993**, *70*, 2313 – 2316.
[15] a) Y. T. Lee, Y. R. Shen, *Phys. Today* **1980**, *33*, 52 – 59; b) P. N. Perera, K. R. Fega, C. Lawrence, E. J. Sundstrom, J. Tomlinson-Phillips, D. Ben-Amotz, *Proc. Natl. Acad. Sci. USA* **2009**, *106*, 12230 – 12234.
[16] a) A. Kusoglu, M. A. Modestino, A. Hexemer, R. A. Segalman, A. Z. Weber, *ACS Macro Lett.* **2012**, *1*, 33 – 36; b) A. Kusoglu, T. K. Cho, R. A. Prato, A. Z. Weber, *Solid State Ionics* **2013**, *252*, 68 – 74; c) Q. Duan, H. Wang, J. Benziger, *J. Membr. Sci.* **2012**, *392 – 393*, 88 – 94.
[17] I. R. Piletic, D. E. Moilanen, D. B. Spry, N. E. Levinger, M. D. Payer, *J. Phys. Chem. A* **2006**, *110*, 4985 – 4999.
[18] a) S. J. Paddison, R. Paul, T. A. Zawodzinski, *J. Electrochem. Soc.* **2000**, *147*, 617 – 626; b) A. Vishnyakov, A. V. Neimark, *J. Phys. Chem. B* **2001**, *105*, 9586 – 9594.
[19] J. R. Kalnin, E. A. Kotomin, J. Maier, *J. Phys. Chem. Solids* **2002**, *63*, 449 – 456.

Received: January 8, 2016
Revised: February 2, 2016
Published online: February 19, 2016

